JOURNAL OF SOLID STATE CHEMISTRY **13**, 231–236 (1975)

New Nonstoichiometric Molybdate, Tungstate, and Vanadate Catalysts with the Scheelite-Type Structure

A. W. SLEIGHT, K. AYKAN,* AND D. B. ROGERS

Central Research Department,† E. I. du Pont de Nemours and Company, Wilmington, Delaware 19898

Received June 10, 1974

Phases of the formula $A_{1-x}\phi_xMO_4$ with the scheelite-type structure are described where ϕ represents a vacancy at the A cation site and M is Mo^{6+}, W^{6+}, and/or V^{5+}. Many different univalent, divalent, and trivalent A cations were used in this study. The phases with no defects, i.e., $x = 0$, were known except for those of the type $A^{1+}_{.5}A^{3+}_{.5}MO_4$ where A^{1+} is Ag or Tl and M is Mo^{6+} or W^{6+}. Phases with $x > 0$ are generally new and were prepared for catalytic studies. An excellent correlation between catalytic properties and defect concentration has been observed.

Introduction

The ideal formula for compounds with the scheelite ($CaWO_4$) structure is AMO_4 where the M cation is tetrahedrally coordinated by oxygen. Since the tetrahedra are not linked, one may view the structure as made up of A cations and MO_4 anions which together take on a cubic close packed arrangement (*1*). The A cation is coordinated to eight oxygens from eight different MO_4 tetrahedra.

Departures from the ideal stoichiometry in the form of A cation deficiencies have been reported for the scheelite structure (*2–4*). The system $Bi_{1-x}\phi_xV_{1-3x}Mo_{3x}O_4$ has been very briefly described by Cesari et al. (*3*), and Chang (*4*) has reported on the systems $Ca_{1-3x}La_{2x}\phi_xWO_4$ and $Ca_{1-3x}Sm_{2x}\phi_xWO_4$.

Many $A_2^{3+}(MO_4)_3$ molybdates and tungstates have scheelite related structures. These phases might be regarded as defect scheelites in the sense that one-third of the A cations are missing. However, the A cation vacancies are generally ordered, and ordered vacancies are actually not defects. There is no long range ordering of the vacancies in the scheelites described in this paper, thus, they are true defect phases.

This work on defect scheelites was undertaken to study the relationship between defects and catalytic properties. A preliminary account has been given (*5*), and a detailed description of the catalytic studies will appear elsewhere (*6, 7*).

Experimental

Phases were prepared from intimate mixtures of reagent grade or better reactants, e.g., PbO, Bi_2O_3, and MoO_3. These were generally heated in air using alumina boats; however, phases containing Tl^+ were prepared in sealed evacuated gold containers. The products were air quenched from the reaction temperature.

Since weight losses during synthesis were negligible, no chemical analyses were performed. X-ray powder patterns were obtained at 25°C using a Hägg-Guinier camera with $CuK\alpha_1$ radiation and an internal standard of high purity KCl ($a = 6.2931$ Å at 25°C). Cell dimensions were refined by least squares. Densities were determined using a pycnometer.

---

* Present address: Research and Development Department, Engelhard Industries Division, Engelhard Minerals and Chemicals Corp., Menlo Park, Edison, N.J. 08817.

† Contribution No. 2160.

TABLE I

DATA FOR SOME SCHEELITE PHASES

Formula	Vacancy concentration	a (Å)	c (Å)	Preparation temperature (°C)
$PbMoO_4$	0.000	5.435	12.109	700–1000
$Pb_{.985}Bi_{.01}MoO_4$	0.005	5.435	12.105	700–900
$Pb_{.97}Bi_{.02}MoO_4$	0.01	5.433	12.100	700–900
$Pb_{.94}Bi_{.04}MoO_4$	0.02	5.429	12.091	700–800
$Pb_{.91}Bi_{.06}MoO_4$	0.03	5.426	12.082	700–800
$Pb_{.88}Bi_{.08}MoO_4$	0.04	5.424	12.072	700–800
$Pb_{.85}Bi_{.10}MoO_4$	0.05	5.420	12.062	700
$Pb_{.82}Bi_{.12}MoO_4$	0.06	5.416	12.055	700
$Pb_{.79}Bi_{.14}MoO_4$	0.07	5.412	12.046	700
$Pb_{.70}Bi_{.20}MoO_4$	0.10	5.400	12.018	700
$Pb_{.74}Bi_{.24}MoO_4$	0.12	5.391	12.000	700
$Pb_{.55}Bi_{.30}MoO_4$	0.15	5.377	11.979	700
$Pb_{.92}Ce^{4+}_{.04}MoO_4$	0.04	5.430	12.084	900
$Pb_{.88}Ce^{3+}_{.08}MoO_4$	0.04	5.433	12.094	900
$Pb_{.87}La_{.087}MoO_4$	0.043	5.431	12.088	800
$Pb_{.4}La_{.4}MoO_4$	0.200	5.405	12.040	900
$La_{.667}MoO_4$	0.333	5.365	11.945	1025
$CdMoO_4$	0.000	5.154	11.192	600
$Cd_{.870}Bi_{.087}MoO_4$	0.043	5.169	11.243	600
$CaMoO_4$	0.000	5.226	11.432	800
$Ca_{.870}Y_{.087}MoO_4$	0.043	5.221	11.408	800
$Ca_{.88}Bi_{.08}MoO_4$	0.040	5.228	11.441	525
$SrMoO_4$	0.000	5.394	12.019	1000
$Sr_{.88}Bi_{.08}MoO_4$	0.040	5.389	11.990	900
$PbWO_4$	0.000	5.462	12.048	800
$Pb_{.97}Bi_{.02}WO_4$	0.01	5.459	12.043	800
$Pb_{.91}Bi_{.06}WO_4$	0.03	5.454	12.030	800
$Pb_{.82}Bi_{.12}WO_4$	0.06	5.447	12.014	800
$Li_{.50}Bi_{.50}MoO_4$	0.000	5.222	11.469	625
$Li_{.44}Bi_{.52}MoO_4$	0.040	5.226	11.502	625
$Li_{.38}Bi_{.54}MoO_4$	0.080	5.232	11.530	625
$Li_{.32}Bi_{.56}MoO_4$	0.120	5.241	11.579	625
$Na_{.50}Bi_{.50}MoO_4$	0.000	5.278	11.585	625
$Na_{.44}Bi_{.52}MoO_4$	0.040	5.276	11.595	625
$Na_{.38}Bi_{.54}MoO_4$	0.080	5.276	11.616	625
$Na_{.32}Bi_{.56}MoO_4$	0.120	5.276	11.638	625
$Ag_{.50}Bi_{.50}MoO_4$	0.000	5.290	11.642	600
$Ag_{.44}Bi_{.52}MoO_4$	0.040	5.287	11.656	600
$Ag_{.38}Bi_{.54}MoO_4$	0.080	5.285	11.668	600
$Ag_{.35}Bi_{.55}MoO_4$	0.100	5.284	11.678	600
$Ag_{.32}Bi_{.56}MoO_4$	0.120	5.283	11.680	600
$Ag_{.29}Bi_{.57}MoO_4$	0.140	5.282	11.690	600
$Ag_{.50}La_{.50}MoO_4$	0.100	5.355	11.740	600
$Ag_{.32}La_{.56}MoO_4$	0.120	5.350	11.790	600
$Tl_{.50}La_{.50}MoO_4$	0.000	5.485	12.454	700
		$b = 5.427$	$\gamma = 90.41°$	
$Tl_{.26}La_{.58}MoO_4$	0.160	5.469	12.316	700
		$b = 5.388$	$\gamma = 90.35°$	
$Ag_{.50}Bi_{.50}WO_4$	0.000	5.304	11.605	800

TABLE I—*continued*

Formula	Vacancy concentration	a (Å)	c (Å)	Preparation temperature (°C)
$Ag_{.50}La_{.50}WO_4$	0.00	5.379	11.701	800
$BiVO_4$	0.000	5.196	11.704	700–900
		$b = 5.093$	$\gamma = 90.38°$	
$Bi_{.99}V_{.97}Mo_{.03}O_4$	0.010	5.189	11.696	800
		$b = 5.099$	$\gamma = 90.30°$	
$Bi_{.98}V_{.94}Mo_{.06}O_4$	0.020	5.182	11.685	800
		$b = 5.111$	$\gamma = 90.22°$	
$Bi_{.97}V_{.91}Mo_{.09}O_4$	0.030	5.176	11.681	800
		$b = 5.121$	$\gamma = 90.17°$	
$Bi_{.95}V_{.85}Mo_{.15}O_4$	0.050	5.159	11.678	800
$Bi_{.93}V_{.79}Mo_{.21}O_4$	0.070	5.155	11.686	800
$Bi_{.90}V_{.70}Mo_{.30}O_4$	0.10	5.175	11.688	700
$Bi_{.85}V_{.55}Mo_{.45}O_4$	0.15	5.191	11.692	700
$Bi_{.9}V_{.7}W_{.3}O_4$	0.10	5.159	11.667	700

Results

Some of the compositions prepared in this study are shown in Table I where the synthesis temperatures are indicated. The products were either white or yellow in color. The refined cell dimensions are also given in Table I. Generally, the phases have the tetragonal symmetry of the ideal scheelite structure, but for some there is a monoclinic distortion.

Some observed and calculated densities are compared in Table II. The observed densities agree well with those calculated on the assumption of A cation vacancies. If the A cation site is assumed to be fully occupied and there are instead interstitial MO_4 groups, the densities (d_i) would be much greater than those observed. Of course, such interstitials are very unlikely for structural reasons.

A phase diagram for the $Pb_{1-3x}Bi_{2x}\phi_xMoO_4$ system (Fig. 1) was constructed from DTA and quenching experiments. The maximum value of x for a single phase scheelite is about 0.15. No solubility of $PbMoO_4$ in $Bi_2(MoO_4)_3$ could be detected. Although the composition $Pb_{.55}Bi_{.30}\phi_{.15}MoO_4$ is only thermodynamically stable close to 700°C, it is readily obtained

TABLE II

DENSITY COMPARISONS[a]

Formula	d_v	d_{obsd}	d_i
$Na_{.50}Bi_{.50}MoO_4$	5.679	5.68	5.679
$Na_{.44}Bi_{.52}\phi_{.04}MoO_4$	5.736	5.75	5.975
$Na_{.38}Bi_{.54}\phi_{.08}MoO_4$	5.783	5.79	6.286
$Na_{.32}Bi_{.56}\phi_{.12}MoO_4$	5.829	5.83	6.624
$Li_{.50}Bi_{.50}MoO_4$	5.690	5.76	5.690
$Li_{.44}Bi_{.52}\phi_{.04}MoO_4$	5.744	5.80	6.014
$Li_{.38}Bi_{.54}\phi_{.08}MoO_4$	5.796	5.81	6.300
$Li_{.32}Bi_{.56}\phi_{.12}MoO_4$	5.831	5.85	6.626
$Pb_{.7}Bi_{.2}\phi_{.1}MoO_4$	6.571	6.55	7.301

[a] d_v is the density calculated on a vacancy model, and d_i is the density calculated on an interstitial model.

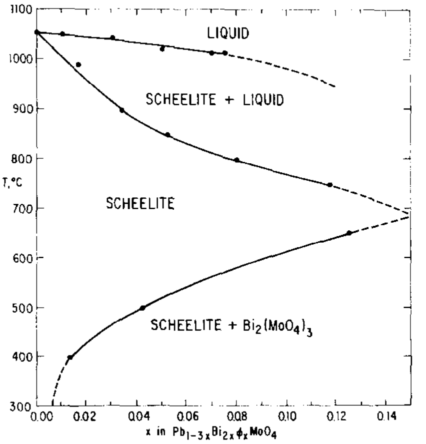

FIG. 1. Phase diagram for the $Pb_{1-3x}Bi_{2x}\phi_xMoO_4$ system.

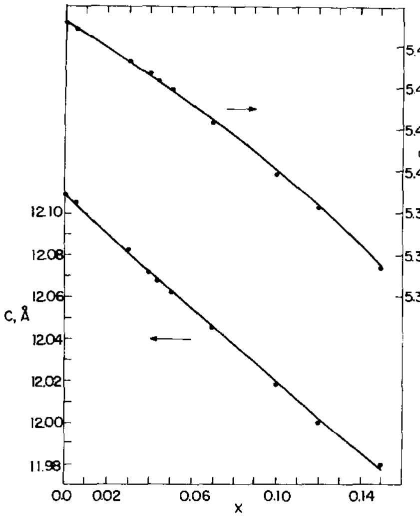

FIG. 2. Cell dimensions vs x in the $Pb_{1-x}Bi_{2x}\phi_xMoO_4$ system.

at room temperature by air quenching. The cell dimensions are plotted as a function of x in Fig. 2. Both a and c decrease in a monotonic fashion as x increases. This decrease is expected since Bi^{3+} is considerably smaller than Pb^{2+}.

Several other systems (Table I) of the type $A^{2+}_{1-3x}A^{3+}_{2x}\phi_xMO_4$ were briefly examined where A^{2+} can be Ca, Sr, Ba, Cd, or Pb; A^{3+} can be Bi or a rare earth; and M is Mo or W. Complete phase diagrams were not determined for these systems, but in the case of the $Pb_{1-3x}La_{2x}\phi_xMoO_4$ system, x can apparently go all the way to 0.333, i.e., $La_2(MoO_4)_3$ (*8*).

Scheelites of the type $A^{1+}_{.5}A^{3+}_{.5}M^{6+}O_4$ are well known as molybdates and tungstates (*9*) where A^{1+} may be Li, Na, or K. We have prepared phases of this type with A^{1+} as Ag or Tl for the first time. The Tl^{1+} compounds cannot be heated in air without oxidation of the Tl^{1+} to Tl^{3+}; however, the Ag compounds are rather stable.

Defect scheelites of the type $A^{1+}_{.5-3x}A^{3+}_{.5+x}\phi_{2x}$-$M^{6+}O_4$ were prepared for the first time. The cell dimensions and volumes are plotted in Figs. 3 and 4 for the systems $A^{1+}_{.5-3x}Bi^{3+}_{.5+x}\phi_{2x}$-$MoO_4$, where A^{1+} is Li, Na, or Ag. Complete phase diagrams were not determined in these systems, but a partial phase diagram is given for the $Li_{.5-3x}Bi_{.5+x}\phi_{2x}MoO_4$ system in Fig. 5.

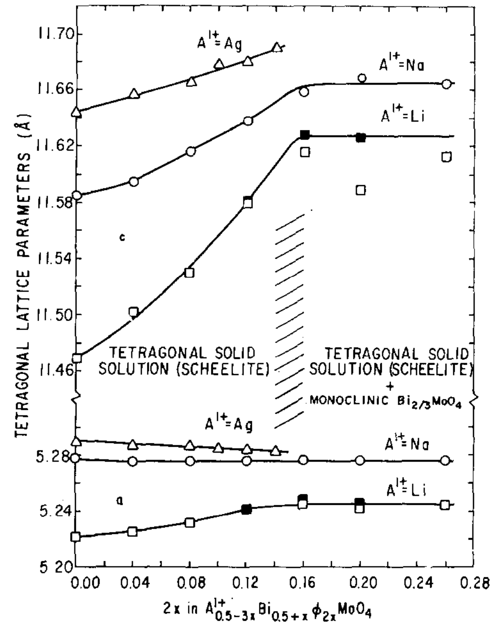

FIG. 3. Cell dimensions vs x in the $A^{1+}_{.5-3x}A^{3+}_{.5+x}\phi_{2x}$-$MoO_4$ systems.

At 600°C the maximum vacancy content ($2x$ in this case) is again about 0.15 for A^{+1} = Li, Na, or Ag. No solubility of the phases in $Bi_2(MoO_4)_3$ could be detected.

Systems based on $BiVO_4$ present a special

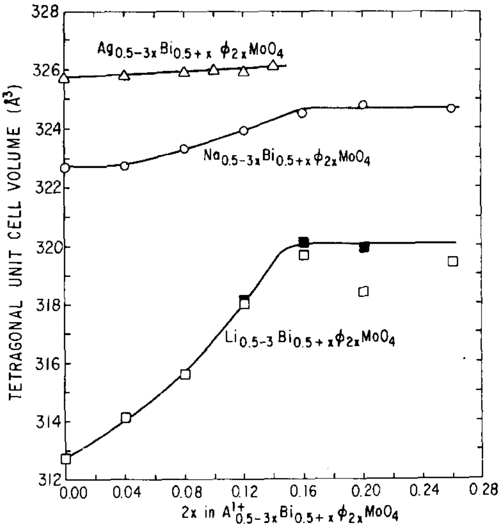

FIG. 4. Cell volume vs x in the $A^{1+}_{.5-3x}A^{3+}_{.5+x}\phi_{2x}MoO_4$ systems.

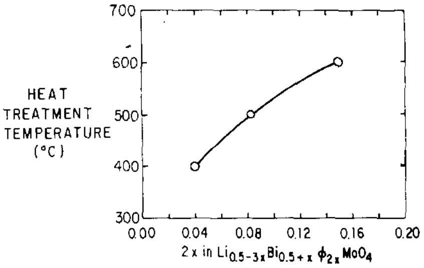

FIG. 5. Temperature vs maximum value of x in $Li_{.5-3x}A^{3+}_{.5+x}\phi_{2x}MoO_4$.

case since scheelite related $BiVO_4$ is monoclinic at room temperature (*10*). The variation in cell dimensions with vacancy concentration is shown in Fig. 6 for the $Bi_{1-x}\phi_xV_{1-3x}Mo_{3x}O_4$ system. At room temperature the symmetry changes from monoclinic to tetragonal at about $x = 0.04$. An analogous $Bi_{1-x}\phi_xV_{1-3x}W_{3x}O_4$ system also exists up to at least $x = 0.10$.

Catalytic Properties

Since detailed catalytic studies are being reported elsewhere (*6*, *7*), only a summary is presented here. Selective oxidation reactions which have been studied are: methanol to formaldehyde, glycol to glyoxal, propylene to acrolein, ammonia and propylene to acrylonitrile, butene to butadiene, and butadiene to furan. Good catalytic activity and selectivity has been observed when the A cation site is partially vacant and partially occupied by bismuth.

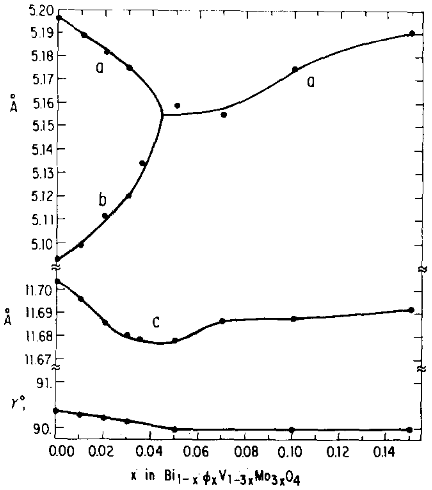

FIG. 6. Cell dimensions vs x in the $Bi_{1-x}\phi_xV_{1-3x}MoO_4$.

The scheelite system studied most extensively was $Pb_{1-3x}Bi_{2x}\phi_xMoO_4$. When there are no defects (i.e., $x = 0$), essentially no activity for the ammoxidation of propylene was observed. However, when $x = 0.005$, good catalytic activity is found, and this activity increases with increasing x. The selectivity is also high, e.g., 75% yields of acrylonitrile can be obtained with 99% consumption of the propylene. Similar results were obtained for other reactions and for tungstates and vanadates.

A study of the $Na_{.5-3x}Bi_{.5+x}\phi_{2x}MoO_4$ system (*5*, *6*) showed that the nondefect phase (i.e., $x = 0$) was relatively inactive even though there was a large amount of bismuth present. Again, the activity increased rapidly as the defect concentration (x) was increased. In the system $Pb_{1-3x}La_{2x}\phi_xMoO_4$, the activity increased with increasing x but not as fast as when bismuth was present, and the selectivity was poor. Thus, the presence of both defects and bismuth is essential for the best catalytic behavior.

Discussion

A large number of vacant A cation sites can be tolerated in the scheelite structure. Chang (*4*) has found that about 25% of these sites can be vacant in the systems $Ca_{1-3x}La_{2x}\phi_xWO_4$ and $Ca_{1-3x}Sm_{2x}\phi_xWO_4$. We find that the limit is about 15% in some systems but as high as 33% in others. As expected, there is a strong temperature dependence for the maximum defect concentration which is thermodynamically stable.

Chang (*4*) has also indicated that there is considerable solubility of the $CaWO_4$ in monoclinic $La_2(WO_4)_3$ and $Sm_2(WO_4)_3$. This is contrary to our observations in other systems. In no case could we detect any solubility of a scheelite $A^{2+}M^{6+}O_4$, $A^{3+}M^{5+}O_4$, or $A^{1+}_{.5}A^{3+}_{.5}$-MO_4 phase in a monoclinic $A_2(MO_4)_3$ phase. Significant solubility of this type would be surprising since A cation vacancies in the monoclinic $A_2(MO_4)_3$ phases are ordered. A change in the concentration of vacancies should quickly destroy their particular ordered arrangement.

Some structural rearrangement might well be expected in the vicinity of A cation vacancies. In fact, the structural work reported for monoclinic $Sm_2(MoO_4)_3$ indicated that the average Mo–O distances were longer than expected for a $(MoO_4)^{2-}$ tetrahedron (*11*). However, that structural refinement was based on a subcell rather than the true cell. A recent refinement (*12*) of monoclinic $La_2(MoO_4)_3$, which has the same structure as $Sm_2(MoO_4)_3$, shows normal Mo–O distances. Furthermore, the structure of $La_2(MoO_4)_3$ shows that there is in fact very little rearrangement of the structure in the vicinity of the vacancies or elsewhere. Thus, in the defect systems we have studied, there is no reason to suppose that there is a substantial structural alteration in the vicinity of the A cation vacancies.

The question of how the introduction of defects into these phases has affected their catalytic properties has not been resolved. It does not appear that the bulk electronic properties have been altered in any way which would affect the catalytic properties. These phases are generally electrically insulating with and without defects (*5*). However, the introduction of defects into the bulk will cause certain defects to appear at the surface. These surface defects may then act as active sites for a catalytic reaction. Thus, by controlling the type and concentration of defects in the bulk, one can hope to control the catalytic activity and selectivity.

It has frequently been shown that doping a material to make it a *p*-type semiconductor results in entirely different catalytic behavior than *n*-type doping (*13*). It has been argued that this shows a relationship between catalytic properties and the electronic structure of a phase. However, it is likely that most *p*-type dopants will give rise to one type of surface defect and *n*-type dopants to another type of surface defect. The electronic properties may not be directly related to the observed catalytic properties. In some cases, the important variables will be the type and concentration of surface defects.

References

1. A. W. SLEIGHT, *Acta Cryst.* **B28**, 2899 (1972).
2. K. NASSAU AND G. M. LOIACONO, *J. Phys. Chem. Solids* **24**, 1503 (1963).
3. M. CESARI, G. PEREGO, A. ZAZZETTA, G. MANARA, AND B. NOTARI, *J. Inorg. Nucl. Chem.* **33**, 3595 (1971).
4. L. L. Y. CHANG, *J. Inorg. Nucl. Chem.* **31**, 2003 (1969).
5. K. AYKAN, A. W. SLEIGHT, AND D. B. ROGERS, *J. Catal.* **29**, 185 (1973); and U.S. Patent No. 3,806,470 (1974).
6. K. AYKAN, D. HALVORSON, A. W. SLEIGHT, AND D. B. ROGERS, *J. Catal.* **35**, 401 (1974).
7. W. LINN AND A. W. SLEIGHT, to be published.
8. L. H. BRIXNER, A. W. SLEIGHT, AND M. S. LICIS, *J. Solid State Chem.* **5**, 247 (1972).
9. L. G. SILLEN AND H. SUNDVALL, *Arkiv Kemi Min eral. Geol.* **17A**, No. 10 (1943),
10. R. S. ROTH AND J. L. WARING, *Amer. Mineral.* **48**, 1348 (1963).
11. P. B. JAMIESON, S. C. ABRAHAMS, AND J. L. BERNSTEIN, *J. Chem. Phys.* **50**, 86 (1969).
12. W. JEITSCHKO, *Acta Cryst.* **B29**, 2074 (1973).
13. For example, see Th. Wolkenstein, *Adv. Catal.* **12**, 189 (1960).